

Design of multi-phase and catalytic chemical reactors: a simulation tool for pollution prevention

Jack R. Hopper, Jamal M. Saleh, Ralph Pike

92:

Abstract A comprehensive chemical reactor analysis tool was required to complete a project to develop an advanced on-line process optimization analysis system for pollution prevention. The advanced process analysis system integrates programs (reactors, on-line optimization pinch analysis, and process flow-sheeting) to analyze and modify chemical processes for waste minimization. The reactor analysis program is to be used to evaluate and analyze multi-phase and catalytic reactors to budget the plant and process engineers the best reactor type and operating conditions. A multi-phase catalytic reactor design and analysis tool, ReaCat, has been developed. ReaCat incorporates models to design the following reactor types: plug flow, CSTR, batch, catalytic fixed-bed, catalytic fluidized-bed, gas-liquid stirred tank, trickle-bed, three-phase fixed bubble-bed, bubble slurry column, CSTR slurry, and three-phase fluidized-bed. This paper gives a summary of the multi-phase and catalytic reactors: classifications, theory and design models, numerical methods, and solution algorithms. A description of the reactor analysis tool including comparison cases with experimental data is presented.

List of Symbols

A Heat transfer area (m^2)
 $C_{G,i}$ Gas bulk concentration of component i (mol/l)
 $C_{G,i}^{in}$ Inlet bulk gas concentration of component i (mol/l)
 $C_{G,i}^{ob}$ Outlet bulk gas concentration of component i (mol/l)
 $C_{L,i}$ Liquid bulk concentration of component i (mol/l)
 $C_{L,i}^{in}$ Inlet bulk liquid concentration of component i (mol/l)

$C_{L,i}^{ob}$ Outlet bulk liquid concentration of component i (mol/l)
 $C_{S,i}$ Concentration of component i at catalytic surface (mol/l)
 C_{pgb} Specific heat capacity of gas ($BTU/°F lb$) [cal/Kg]
 C_{plb} Specific heat capacity of liquid ($BTU/°F lb$) [cal/Kg]
 D_{Ab} Bulk diffusivity (cm^2/s)
 $D_{L,i}$ Liquid-phase axial dispersion coefficient (cm^2/s)
 E Energy of activation (kJ/mol)
 F Flow rate of gas (m^3/s)
 F_i^{gasb} Inlet flow rate for component i
 F_i^{lib} Heat of reaction of component i (kJ/mol)
 ΔH_{ri} Henry's constant for component i
 H_i First-order reaction constant
 K Gas-phase (bubble-phase) mass transfer coefficient ($1/s$)
 K_{BCb} Intermediate (cloud-wake) phase mass transfer coefficient ($1/s$)
 K_{CEb} Liquid-solid mass transfer coefficient ($1/s$)
 K_{cbcb} Gas-liquid mass transfer coefficient for component i ($1/s$)
 $(K_{Lbg})_i$ Liquid-solid mass transfer coefficient for component i ($1/s$)
 $(K_{cbc})_i$ Gas-phase mass transfer coefficient ($1/s$)
 K_{gbLb} Liquid-phase mass transfer coefficient ($1/s$)
 K_{LbLb} First-order reaction constant
 N Number of species in mixture
 P_i^{in} Inlet bulk gas partial pressure of component i [(psi) bar]
 P_i^{ob} Outlet bulk gas partial pressure of component i [(psi) bar]
 Q_{Gb} Gas volumetric flow rate (cm^3/s)
 Q_{Lb} Liquid volumetric flow rate (cm^3/s)
 Q_{Gmaxb} Maximum gas flow rate (cm^3/s)
 R Gas constant ($l atm/mol K$)
 $(-r_i)$ Net rate of disappearance of component i
 t Time (s)
 T_{ib} Inlet temperature [$°F$] [K]
 T_{ob} Outlet temperature [$°F$] [K]
 T_{ab} Ambient temperature [$°F$] [K]
 U Overall heat transfer coefficient [$BTU/h ft^2 °F$] [$cal/s cm^2 K$]
 U_{Gb} Gas superficial velocity (cm/s)
 U Bulk gas-phase velocity (cm/s)
 U_{Lb} Liquid superficial velocity (cm/s)
 V_{Rb} Reactor volume (m^3)
 V_{Tb} Volume of reservoir (m^3)

Received: 20 January 2000 / Accepted: 2 April 2001
 Published online: 10 July 2001
 © Springer-Verlag 2001

J. R. Hopper (✉), J. M. Saleh
 Lamar University, Chemical Engineering Department,
 P.O. Box 10053, Beaumont, TX 77710, USA
 E-mail: jhopperjr@hal.lamar.edu

R. Pike
 Louisiana State University, Baton Rouge, Louisiana, USA

Support from the Gulf Coast Hazardous Substance Research Center and the Environmental Protection Agency is gratefully acknowledged

z Axial position (cm)
 ρ_L Density of liquid (g/cm^3)
 τ Gas-space time (V_R/Q_G) (s)

8. Multi-reaction systems with up to 30 reactions and 36 components
 9. Prediction of reactor hydrodynamics such as preure drop, power consumption, catalyst-wetting factor, and flow regimes.

Introduction

To perform an advanced process system analysis, which is used to evaluate chemical and refinery processes for waste minimization (Telang 1996, Pike et al. 1998), an advanced chemical reactor tool is essential. The reactor design tool is to be used to evaluate and analyze the various types of industrial multi-phase and catalytic reactors. In an effective and time-saving manner, plant and process engineers need a reactor design tool to analyze and study the effect of operating conditions on the pollution index. For this purpose, ReaCat, a multi-phase catalytic reactor analysis simulation tool, has been developed with the following features:

1. User-friendly input/output interface
2. Graphical and tabular data output
3. Reactor models included
 - ib Homogeneous reactors (plug flow, CSTR, batch)
 - iib Heterogeneous reactors
 - I Catalytic gas fixed-bed
 - II Catalytic liquid fixed-bed
 - III Catalytic gas fluidized-bed
 - IVb Catalytic liquid fluidized-bed
 - Vb Gas-liquid continuous stirred tank
 - VI Three-phase trickle-bed
 - VII Three-phase bub le fixed-bed
 - VIII Three-phase catalytic gas-liquid slurry stirred tank
 - XI Three-phase catalytic gas-liquid slurry bub le-bed
 - Xb Three-phase catalytic gas-liquid fluidized-bed
4. Power-law reaction rate or the Langmuir-Hinshelwood model to account for the catalytic adsorption effects
5. Equipped with correlation to estimate the external mass transfer effects (gas-liquid, and liquid-solid), and dispersion coefficients
6. Estimation of the catalytic effectiveness factor to account for the intra-particle resistance
7. Isothermal and non-isothermal/non-adiabatic conditions

Multi-phase and Catalytic Reactor, Definitions and Classifications

In industrial chemical processes, multi-phase reactors have a wide range of applications such as oxidation, hydrogenation, hydro-desulfurization, and the Fischer-Tropsch synthesis. Table 1 lists the definition for the different reactor types included in this study. Multi-phase reactors are defined as reactors with at least two distinct phases in contact. Reactors, in general, may be classified based on the number of phase coexistence into the following category:

- i) Homogeneous: one phase such as gas or liquid exists in the reactor. The hydrodynamic flow characteristic of the mixture determines the reactor type such as plug, CSTR, or batch.
- ii) Heterogeneous: two distinct phases of reactants (or catalyst) coexist. This category may be classified into the following subcategories:
 - a) Catalytic reactors: gas or liquid phase (or both) is in contact with a catalyst (mainly solid, but could be another liquid phase). Examples of this category include the catalytic packed-bed (catalytic gas reaction) and the three-phase trickle-bed (catalytic gas-liquid reaction).
 - b) Non-catalytic reactors: gas-liquid or liquid-liquid reactions are carried in a variety of contact vessels such as the gas-liquid continuous stirred tank reactor.

Each reactor type exhibits certain characteristics and advantages that may make it the best candidate for a specific reaction; the power of a simulation tool becomes very clear for such an analysis. For a complete discussion on examples, classification, definitions, and advantages or disadvantages of multi-phase and catalytic industrial reactors, the reader is referred to Ostergaard (1974), Shah (1979), Tarhan (1979), Ramachandran and Chaudhari (1983), Tsutsu et al. (1987), and Saleh (1994).

Table 1.1 Definitions of reactors

Catalytic packed-bed	Gas or liquid reactants flow over a fixed-bed of catalysts
Catalytic fluidized-bed	The up-flow gas or liquid phase suspends the fine catalyst particles
CSTR gas-liquid	Liquid and gas phase are mechanically agitated
Bub le gas-liquid bed	Liquid phase is agitated by the bub le rise of the gas phase. Liquid phase is continuous
Trickle-bed	Concurrent down-flow of gas and liquid over a fixed-bed of catalyst. Liquid trickles down, while gas phase is continuous
Bub le fixed-bed	Concurrent up-flow of gas and liquid. Catalyst bed is completely immersed in a continuous liquid flow while gas rises as bub les
CSTR slurry	Mechanically agitated gas-liquid catalyst reactor. The fine catalyst particles are suspended in the liquid phase by means of agitation. (Batch liquid phase may also be used)
Bub le slurry column	Liquid is agitated by means of the dispersed gas bub les. Gas bub le provides the momentum to suspend the catalyst particles
Three-phase fluidized-bed	Catalyst particles are fluidized by an upward liquid flow while gas phase rises in a dispersed bub le regime

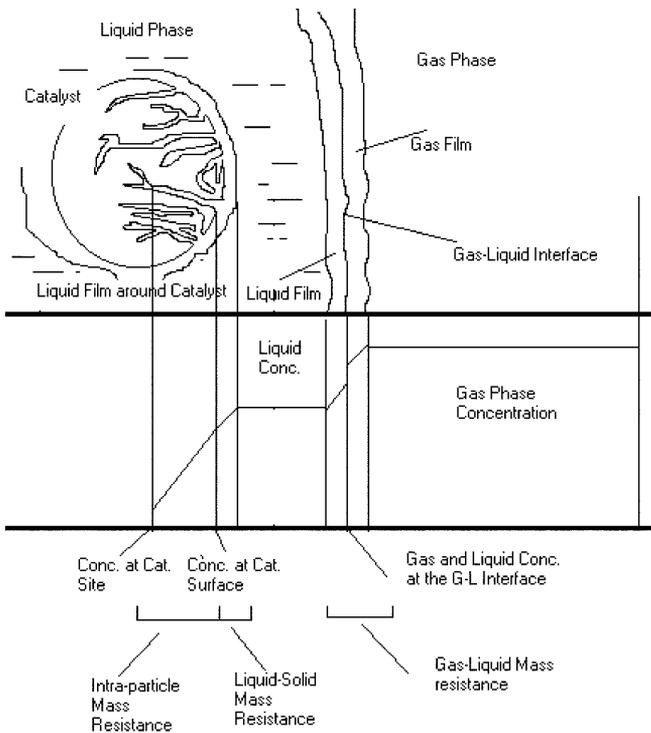


Fig.S1.S Gas-liquid-solid contact in three-phase reactors

Design Models

Design of multi-phase catalytic reactors is more complex than that of homogeneous reactors due to the following: the coexistence of more than one phase introduces the mass transfer resistance (Fig 1), the intra-

particle diffusion, adsorption effects and the flow regimes, which may be different for each phase. The details of the mathematical model, assumptions, and solution algorithm for each of the reactor types are listed in Saleh (1994), Hedge (1999), and Waghchoure (1999). Tables 2, 3, 4, 5, 6, 7 and 8 show the design model, assumptions, and solution algorithms for the three-phase trickle-bed, three-phase catalytic slurry CSTR, and gas-liquid (non-catalytic) agitated tank, catalytic liquid fluidized-bed, catalytic gas fluidized-bed, and catalytic fixed-bed, respectively. The trickle-bed model (Table 2) is applicable to three-phase fixed-bed, three-phase fluidized-bed, and three-phase bubble slurry-bed as well. A complete list of correlations implemented in the ReaCat program to predict the mass transfer and hydrodynamic parameters are listed in Saleh (1994), Hedge (1999), and Waghchoure (1999). The selection of these correlations is based on the recommendation, found in literature review, of other authorities in this area. For example, the correlations implemented for the three-phase reactors are those recommended by Ramachandran and Chaudhari (1983). Since most of the correlations were developed for laboratory and pilot reactors, programs are allowed to skip correlations when experimental data are available. Tables 8 and 9 give a summary of the correlations used in the program. For catalytic reactors, intra-particle diffusion is accounted for by multiplying the intrinsic reaction rate by the catalytic effectiveness factor. The procedure to estimate the catalytic effectiveness factor is listed in Table 10. Procedures to warn the user of conditions that violate the model assumptions are also included. For example, when the catalytic wetting factor is not unity or when the flow regime

Table 2. S Three-phase gas-liquid catalytic reactors design model (trickle-bed, fixed-up-flow bubble-bed, bubble slurry bed, three-phase fluidized-bed)

Non-volatile liquid-phase mass balance	$D_{L,i} \frac{d^2 C_{L,i}}{dz^2} - U_L \frac{dC_{L,i}}{dz} - (K_c)_i (C_{L,i} - C_{S,i}) = 0.0$	(1)
Volatile liquid-phase mass balance	$D_{L,i} \frac{d^2 C_{L,i}}{dz^2} - U_L \frac{dC_{L,i}}{dz} + (K_L)_{gi} \left(\frac{C_{G,i}}{H_i} - C_{L,i} \right) - (K_c)_i (C_{L,i} - C_{S,i}) = 0.0$	(2)
Boundary conditions	$At z = 0: -D_{L,i} \frac{dC_{L,i}}{dz} = U_L (C_{L,i} - C_{L,i}^i)$ $At z = L: \frac{dC_{L,i}}{dz} = 0$	
Gas-phase mass balance	$-U_g \frac{dC_{G,i}}{dz} - (K_L)_{gi} \left(\frac{C_{G,i}}{H_i} - C_{L,i} \right) = 0.0$	(3)
Component mass balance around the catalyst	$(K_c)_i (C_{L,i} - C_{S,i}) = (-r_i)$	(4)

Model assumptions

1. Complete radial mixing
2. Axial backmixing is accounted for by the dispersion parameter
3. Gas and liquid concentration and temperature profiles are function of reactor length only
4. Complete catalyst wetting factor and uniform catalyst concentration and activity
5. The catalytic effectiveness factor accounts for the intra-particle diffusion resistance

Solution algorithm

1. Equations 1-4 are developed for each component in mixture
2. At the inlet of reactor, $z=0$, the nonlinear algebraic system of Eq. 4 is solved for the concentration at the catalyst surface by the Newton-Raphson numerical method
3. When plug flow model is assumed, Eqs. 2, 3, and 4 are integrated using the previously calculated surface concentration. For the dispersion model, the shooting method is applied
4. Steps 1-3 are repeated for the entire reactor length

developed is better than the assumed, a warning message will be displayed at the end of the calculation. Each of the mathematical models has been tested versus other published experimental or simulation work. Table 11 lists some comparison examples; for more examples the reader may refer to Salehi (1994).

Program Description

A user-friendly input/output program has been developed to solve and analyze the different reactor types. Figures 2, 3, and 4 show a few of the input screens. A complete user manual may be requested from the authors. Results may be viewed in graphical or tabular format. The user can view conversion, concentration, temperature, and pressure, which may be displayed as a function of reactor length, volume, catalyst weight, or reaction time (Fig 5).

Another version of React was built to allow simple flow heating capability, such as connecting reactors in series or parallel, generic mixing and splitting of streams, and generic heat transfer equipment (Fig 6).

Example E1, Sulfuric Acid Production by Contact Process

The production of sulfuric acid by the contact process is a three-step process that produces sulfuric acid and steam from air, molten sulfur, and water. The process consists of three sections: (1) the feed preparation section; (2) the reactor section; (3) the absorber section. The feed preparation section, molten sulfur feed is combusted with dry air in the sulfur burner to produce SO₂. The reaction section is the reactor or converter section. Gases from the feed section, sulfur dioxide and air, enter at (787°F) 419.4°C and (19.4 bPa) 13,759.12 bPa. Sulfur dioxide and

Table 3.3 Three-phase gas-liquid catalytic reactors design model (CSTR blurry)

Non-volatile component liquid-phase mass balance	$Q_L(C_{L,i}^{ib} - C_{L,i}^{ob}) - V_R(K_c)_{cb,i}(C_{L,i}^{ob} - C_{S,i}) = 0.0$	(1)
Non-volatile component liquid-phase mass balance	$Q_L(C_{L,i}^{ib} - C_{L,i}^{ob}) + V_R(K_L)_{gb,i}(C_{G,i}^{ob} - C_{L,i}^{ob}) - V_R(K_c)_{cb,i}(C_{L,i}^{ob} - C_{S,i}) = 0.0$	(2)
Gas-phase mass balance	$Q_G(C_{G,i}^{ib} - C_{G,i}^{ob}) - V_R(K_L)_{gb,i}(C_{G,i}^{ob} - C_{L,i}^{ob}) = 0.0$	(3)
Component mass balance around the catalyst	$V_R(K_c)_{cb,i}(C_{L,i}^{ob} - C_{S,i}) = V_R(-r_i)$	(4)

Model assumption

1. Gas and liquid phases are well agitated
2. Uniform concentration and temperature within each phase in the entire reactor volume
3. Complete and homogeneous catalyst suspension
4. Continuous flow

Solution algorithm

1. Equations 1-4 are developed for each component in mixture
2. An initial guess for the surface concentration is assumed
3. For a given reactor volume, the system of nonlinear algebraic equations is solved iteratively by the Newton-Raphson method to find the exit conditions

Table 3.4 Gas-liquid agitated tank design model

Gas-phase component mass balance	$(Q_G/RT)(P^i - P^o) + V_R E K_G (P^o/H_i - C_{Li}^{ob}) = 0$	(1)
or	$F_{gas} P_T (P^i - P^o) - V_R E K_G (P^o/H_i - C_{Li}^{ob}) = 0$	
Liquid-phase volatile-component mass balance	$Q_L(C_{Li}^{ib} - C_{Li}^{ob}) + V_R E K_L (P^o/H_i - C_{Li}^{ob}) + r_i V_R = 0$	(2)
Liquid-phase non-volatile-component mass balance	$Q_L(C_{Li}^{ib} - C_{Li}^{ob}) + r_i V_R = 0$	(3)
Energy balance	$\sum F^i i [\alpha_i(T_i - T_o) + \beta_i/2(T_i^{2b} - T_o^{2b}) + \gamma_i/3(T_i^{3b} - T_o^{3b})] - [V_R \sum (\Delta H_{ri} r_i)] + UA(T_a - T_o) = 0$	(4b)

Model assumption

1. Steady state
2. Both phases are assumed to be perfectly macro-mixed
3. Uniform gas and liquid temperature

Solution algorithm

1. Provide an initial guess for the design variables: gas and liquid concentration and temperature
2. Estimate the hydrodynamic parameters: mass transfer coefficients, power consumption, and minimum gas flow rate
3. Equations 1-4 are developed for each component in mixture
4. The system of nonlinear algebraic equations is solved simultaneously by the Newton-Raphson method

oxygen from air react with each other to produce SO_3 and react with water to form sulfuric acid. In the actual process since this is an exothermic reaction, SO_3 from the reactor section is passed to the absorber section where it is possible to convert with intermediate removal of heat and

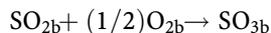
Table 5.5 Catalytic liquid fluidized-bed reactor, design model

Liquid-phase component balance	
Plug flow	$-U_L \frac{dC_{iL}}{dZ} = K_L(C_{iL} - C_{iS}) \quad (1)$
Dispersion	$D_{Lb} \frac{d^2 C_{iL}}{dZ^2} - U_L \frac{dC_{iL}}{dZ} = K_L(C_{iL} - C_{iS}) \quad (2)$
Catalyst (emulsion) phase	$K_L(C_{iL} - C_{iS}) = (R)_{iCatalystPhase} \quad (3)$
Energy balance	$\rho_L U_L C_{pL} \frac{dT}{dZ} = \sum_{j=1}^{NR} R_j \Delta H_{rj} + Ua(T_{ambient} - T_{Reactor}) \quad (4)$
Assumptions	
<ol style="list-style-type: none"> The reaction in the liquid phase is assumed negligible By neglecting internal convection effects, the catalyst and the liquid are assumed to be at the same temperature used on the extremely small particle sizes. (in μm) Steady state 	
Solution algorithm	
<ol style="list-style-type: none"> Estimate the required parameters ($U_L, K_L, \text{expanded length of bed}$) Catalyst surface concentration (Eq. 3) are converged using the Newton-Raphson method with the Gauss-Jordan elimination method. As a starting guess, catalyst phase concentration are assumed to be equal to concentrations in liquid phase Liquid concentration (Eq. 1 or 2) for the next interval are calculated depending on type of flow selected. (4th order Runge-Kutta for plug flow, finite difference for the dispersion model) 	

Table 6.5 Catalytic gas fluidized-bed reactor, design model

Design equations	
Bulk (gas phase) (bubble phase) Plug flow	$-U \left(\frac{dC_{iG}}{dZ} \right) = K_{BC}(C_i - C_{iC}) \quad (1)$
With axial dispersion	$D_{gab} \frac{d^2 C_i}{dZ^2} - U \left(\frac{dC_{iG}}{dZ} \right) = K_{BC}(C_i - C_{iC}) \quad (2)$
Intermediate (cloud-wake) phase	$K_{BC}(C_i - C_{iC}) = \chi_{cb}(R)_{iCloudPhase} + K_{CE}(C_{iC} - C_{iE}) \quad (3)$
Catalyst (emulsion) phase	$K_{CE}(C_{iC} - C_{iE}) = \chi_{eb}(R)_{iEmulsionPhase} \quad (4)$
Energy balance	$\rho_g U (C_{pg} \frac{dT}{dZ}) = \sum_{j=1}^{NR} R_j \Delta H_{rj} + Ua(T_{ambient} - T_{Reactor}) \quad (5)$
Assumptions	
<ol style="list-style-type: none"> Three phases present in a gas fluidized-bed reactor. Bulk gas phase is known bubble phase. Intermediate phase contains both gas and the solids. Catalyst (emulsion) phase has solids in higher concentration The gas bubbles formed are assumed to be spherical in nature Mass transfer is believed to be happening in all three phases The reaction occurring in bulk gas (bubble) phase is both significant and hence is neglected Steady state 	
Solution algorithm	
<ol style="list-style-type: none"> Estimate the required parameters using correlations ($D, U, \chi_{cb}, \chi_{eb}, K_{BC}, K_{CE}$) Intermediate and solid surface concentrations (Eqs. 3 and 4) are converged using the Newton-Raphson method with the Gauss-Jordan elimination method Bulk gas concentrations (Eqs. 1 or 2) for the next interval are calculated depending on type of flow selected. (4th order Runge-Kutta for plug flow, finite difference for the dispersion model) For non-isothermal cases, the temperature for the next interval is calculated by Eq. 5 and used to find reaction rates for the next length interval Steps 3 and 4 are repeated over the total reactor length 	

The product, SO₃. The removal increases the equilibrium conversion. The reaction takes place on a vanadium pentoxide catalyst. Two types of this catalyst LP-110 and LP-120 are used in these reactors. The reaction is:



$$r_{\text{SO}_{2b}} = \frac{P_{\text{SO}_2} P_{\text{O}_2b}^{1/2b}}{(A + BP_{\text{O}_2b}^{1/2b} + CP_{\text{SO}_{2b}} + DP_{\text{SO}_{3b}})^2} \left[1 - \frac{P_{\text{SO}_3}}{K_P P_{\text{SO}_2} P_{\text{O}_2}^{1/2b}} \right]$$

The kinetic model for this reaction was given by Harrib and Norman (1972). The reaction rate is predicted by the where

Table 7.5 Catalytic fixed-bed, design model

Mass balance around the catalyst	$(c_c)_i (C_{Gb} - C_s) i = \eta (-R) i$	(1)
Gas-phase component mass balance (plug flow model)	$-U_G \frac{dC_{Gi}}{dz} - (c_c)_i (C_{Gb} - C_s) i = 0.0$	(2)
Gas-phase component mass balance (dispersion model)	$D_G \frac{d^2 C_{Gi}}{dz^2} - U_G \frac{dC_{Gi}}{dz} - (c_c)_i (C_{Gb} - C_s) i = 0.0$	(3)
Energy model	$U_G \rho_G C_{Pg} \frac{dT}{dz} = \sum (R_j \Delta H_{Rj}) + UA(T - T_a)$	(4)

Model assumption

1. Complete radial mixing
2. Dispersion coefficient is used to account for the axial back mixing
3. Effectiveness factor accounts for the intra-particle resistance
4. Steady state

Solution algorithm

1. At the reactor inlet, develop Eq. for each component in the mixture
2. Solve the system of nonlinear algebraic equations for the concentration at the catalyst surface, C_s. This is an iterative procedure as follows: Guess C_s, solve for the effectiveness factor, evaluate the net intrinsic reaction rate for each component, then using the Newton-Raphson method to solve the system of Eqs. 1, new values for C_s are estimated. The process is repeated till no further change in C_s is occurring
3. Develop Eqs. 2 or 3 (depending on the model choice, plug or dispersion) for each component in mixture; solve for the next increment in reactor length using the 4th order Runge-Kutta method or finite difference
4. Repeat the above steps for the next reactor length increment

Table 8.5 Correlation used for the three-phase catalytic reactors

Correlation	Trickle-bed	Fixed up-flow	CSTR blurry	Bubble blurry	Three-phase fluidized
Pressure drop	Larkins et al. (1961)	Turpin and Hintington (1967)	-	-	-
L and G holdup < 1b	Ellman et al. (1988) Satoh et al. (1973)	Fukushima and Kusak (1979)	Calderbank (1958)	Yamashita and Aeon (1975) Maselker (1970)	Kim et al. (1975)
G-L mass transfer coefficient	Ellman et al. (1988) Satoh et al. (1973)	Achwal and Stepanek (1976)	Bern et al. (1976)	Akita and Yoshida (1974)	Dhanak and Stepanek (1980) Dakshinamurthy et al. (1974)
L-S mass transfer coefficient	Van Krevelen and Kerkels (1948) Dharwadker and Sylvester (1977)	Specchia et al. (1978)	Sanoh et al. (1974)	Kobayashi and Saito (1965)	Lee et al. (1974)
L dispersion coefficient	Michell and Furzer (1972)	Stiegel and Shah (1977)	-	Deckwer et al. (1974)	El-Temtamy et al. (1979)
G dispersion coefficient	Hochman and Effron (1969)	-	-	Mangartz and Pilhofer (1981)	-
Wall heat transfer coefficient	Specchia and Baldi (1979)	-	-	Fair (1967)	-
Power consumption	-	-	Luong and Volesky (1979) Michell and Miller (1962)	-	-

$P_{SO_2}, P_{O_2}, P_{SO_3}$ are interfacial partial pressures of $SO_2, O_2,$ and SO_3 (atm)
 K_p is the thermodynamic equilibrium constant (atm^{-1/2})
 Constants $A, B, C,$ and D are functions of temperature T (P denotes interfacial partial pressures of SO_2 and O_2 at zero conversion under total pressure at the point of reactor (atm))

For catalyst type LP-110

$$A = e^{-6.8+4960/T}, B = 0, C = e^{10.32-7350/T}, D = e^{-7.38+6370/T}$$

For catalyst type LP-120

$$A = e^{-5.89+4060/T}, B = 0, C = e^{6.45-4610/T}, D = e^{-8.59+7020/T}$$

For the heat of reaction, an empirical formula is used, which was also derived by Harris and Norman (1972):

$$\Delta H_{\text{reaction}} = 1.827(-24097 - 0.26T + 1.69 \cdot 10^{-3} T^2 + 1.5 \cdot 10^5 / T) \rightarrow \text{BTU/lbmol (cal/gmol)}$$

The complete list of input parameters and operating conditions provided for the ReaCat Program is given in Kuni and Levenspiel (1969).

Results

An SO_2 conversion of 59.74% is obtained (catalyst type LP-120) at the exit point of the reactor and the outlet temperature is (1014°F) 545.55°C. If LP-110 catalyst is used, 45.99% conversion is obtained with an exit temperature of (950°F) 510°C. It can be seen that conversion is higher for LP-120, hence SO_2 emission will be less. Keeping the catalyst type constant and varying the inlet flow rate shows that decreasing the flow rate increases the conversion thus reducing SO_2 emission. Since this is an exothermic reaction, conversion decreases at higher temperatures. The process uses intermediate coolers to lower the temperature, which gives a better conversion and reduces SO_2 emission.

Example 2, Catalytic Oxidation of Ethanol in Waste Water

Organic pollutant dissolved in liquid water are usually removed by the biological oxidation process. However, some pollutant with aromatic structure decompose slowly under this process. Liquid-phase oxidation of organic pollutant in water with solid catalyst provides a method that may remove dissolved organic compounds. This is a typical case where three-phase reactors are applied since the process contains liquid (aqueous

Table 9.3 Correlation used for the two-phase reactors

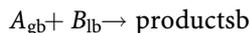
Gas-liquid continuous stirred tank reactor	
1. Maximum gas flow rate (Q_{Gmax})	Charpehier (1981)
2. Bubble diameter (d)	Van Dierendonck (1970)
3. Gas holdup (ϵ_G)	Van Dierendonck (1970)
4. Liquid side mass transfer coefficient (b_L)	Van Dierendonck (1970)
Catalytic liquid fluidized-bed	
Mass transfer coefficient (K_L)	Chubertal (1953)
Catalytic gas fluidized-bed	
1. Voidage at minimum fluidization (ϵ_{mf})	Broadhurst and Becker (1975)
2. Velocity at minimum fluidization (U_{mf})	Kuni and Levenspiel (1969)
3. Bubble diameter (D_B)	Hori and Nonaka (1987)
4. Mass transfer coefficients (K_{BC} and K_{CE})	Kuni and Levenspiel (1969)
5. Coefficient for axial dispersion (D_{GA})	Kuni and Levenspiel (1969)
Catalytic gas fixed-bed	
1. Coefficient for axial dispersion	Kuni and Levenspiel (1969)

Table 10.3 Calculation of catalytic effectiveness factor

Catalytic effectiveness factor	$\eta = \frac{1}{\phi} \left(\coth 3\phi - \frac{1}{3\phi} \right)$ where ϕ is the Thiele modulus
First order reaction rate	
Spherical pellet	$\phi = \frac{R}{3b} \sqrt{k_s a \rho_p / D_e}$
Cylindrical pellet	$\phi = \frac{R}{2b} \sqrt{k_s a \rho_p / D_e}$
Slab pellet	$\phi = L \sqrt{k_s a \rho_p / D_e}$
General non-linear reaction rate where	$\phi = \frac{R}{3} \rho_p (-r(CS)) \left\{ \int_0^{C_{sb}} 2De(-r(CS)) dCS \right\}^{-0.5}$
D_{ekb}	Limiting reactant index
C_{skb}	Effective diffusivity for the limiting reactant
$(-r(C))$	Limiting reactant concentration at catalyst surface
R	Intrinsic reaction rate as non-linear function of surface concentration
ρ_p	Catalyst pellet radius
Limiting reactant is found by the following criterion	Catalyst density
D_{eb}	$D_{eB} C_{SB} > 10 D_{eA} C_{SA}$
C	Stoichiometry of B when stoichiometry of A = 1
	Effective diffusivity
	Surface concentration

organic), gas (oxygen), and solid (catalyst). The objective of this analysis is to compare the ethanol conversion profiles for the different types of the three-phase reactors.

An atypical catalyst used in this reaction is $Pd-Al_2O_3$ at $30^\circ C$. The reaction has been shown to be first order with respect to oxygen and zero order with respect to ethanol. The reaction stoichiometry is represented as:



where

A Oxygen
 B Ethanol
 g Gas phase
 l Liquid phase

The rate constant k , $0.0177 \text{ cm}^3/\text{g}\cdot\text{s}$. Table 1.2 lists other parameters and operating conditions needed to run the ReaCat package. Since fixed-bed and suspended-beds have different characteristics regarding the catalyst load and catalyst particle diameter, different sizes of catalyst particles and catalyst loads were used in fixed-bed and suspended-beds. However, all other parameters and operating conditions are essentially the same in this comparison. Table 1.2 shows the different catalyst and reactor characteristics as used in the study.

Design Models and Solution Algorithms

A dispersion model is used to describe the liquid-phase component material balances in the following reactors: bubble fixed-bed, bubble slurry, and three-

phase fluidized. The gas phase was assumed to move in plug flow. Table 1.2 shows the component balances for the catalyst, gas, and liquid phase for the above reactors. Table 1.3 lists the component material balances in the well-agitated slurry reactor (CSTR slurry).

The catalytic effectiveness factor was calculated according to equations presented in Table 1.0. The gas-liquid and liquid-solid mass transfer coefficients were found using the correlations presented in Table 9. Values calculated for the mass transfer coefficients and catalytic effectiveness factors are given in Table 1.3.

Results and Discussions

The conversion profiles for the fixed-bed (trickle and bubble fixed-bed) and the suspended-bed (slurry and fluidized) reactor groups were compared separately because of the difference in catalyst load and particle size. However, the catalyst load and particle size are the same within each group.

Figure 7 shows the ethanol conversion profiles in the trickle-bed and the bubble fixed-bed. The slight conversion increase in the bubble fixed-bed over the trickle-bed (about 4% at length = 500 cm) is probably due to higher value of bubble fixed-bed mass transfer coefficients. The catalytic effectiveness factor for both of the fixed-bed reactors was found to be 0.13, while dispersion coefficients were negligible for both of these reactors in comparison with those for suspended-beds (Table 1.3).

Figure 8 shows a comparison of the ethanol conversion profiles in suspended-bed reactors. Similar catalyst load and particle diameter were used in the three types of

Table 1.1. ReaCat test cases

Catalytic gas fluidized-bed						
Multiple reaction system for the production of phthalic anhydride from naphthalene (Kunii and Levenspiel)						
Literature	ReaCat(1)	ReaCat(2)	ReaCat	Dispersion		
Conversion	Plug flow	Plug flow	Plug flow	97%	85.49%	81.26%
(1) Experimental bubble diameter values has been used by the program						
(2) The correlation of Horio and Nonaka (1984) has been used to find the bubble diameter						
Continuous gas-liquid stirred tank reactor						
Liquid phase oxidation of o-xylene to o-methylbenzoic acid by means of air (Froment and Bischoff 1979)						
Conversion	Literature	ReaCat				
	83.39%	83.95%				
Trickle-bed						
Liquid-phase oxidation of formic acid in the presence of CuO.ZnO catalyst (Baldib et al. 1974; Gotto and Smith 1975)						
Conversion	Experimental	ReaCat (plug flow)	ReaCat (dispersion)			
	88.5%	91.0%	89.8%			
Continuous catalytic gas-liquid slurry stirred tank reactor						
Hydrogenation of aniline to cyclohexylamine (supported nickel catalyst) (Govindarao and Murthy 1975; Ramachandran and Chaudhari 1983)						
Reactor volume	Literature	ReaCat				
(46% conversion of Aniline)	98 l	99 l				
Semi-batch catalytic gas-liquid slurry stirred tank reactor						
Butyraldehyde synthesis by the reaction of gaseous acetylene with aqueous formaldehyde in the presence of copper acetylacetonate catalysts (Kale et al. 1981)						
Conversion	Experimental	ReaCat(1)	ReaCat(2)			
	62%	61.0%	68.5%			
(1) Adsorption at catalyst surface is taken into account by the program						
(2) No adsorption effects						

REACTION

Gas Homogeneous
<input checked="" type="checkbox"/> Liquid Homogeneous
Catalytic Gas
Catalytic Liquid
Gas-Liquid
Catalytic Gas-Liquid

100: Fig.S2.S Reaction phase menu

REACTOR TYPE

<input checked="" type="checkbox"/> Plug Flow
CSTR
Batch

Fig.S3.S Reactor type menu

suspended-beds. The catalytic effectiveness factor in suspended-beds was found to be much higher than that for fixed-beds (0.799 compared with 0.13 in fixed-beds) due to fine catalyst particles. The conversion profiles for the three-phase fluidized-bed and bubble slurry reactor had values that were very similar. The conversion in the three-phase fluidized-bed was higher by 9% than that in the bubble slurry reactor at length 500 cm. However, the conversion profile for the CSTR slurry reactor was much higher than in either suspended-beds. The conversion of ethanol in CSTR slurry was 52% higher than in the bubble bed and 37% higher than in the three-phase fluidized-bed at length 500 cm. The high conversion in the CSTR slurry reactor can be explained by the much higher mass transfer coefficients due to the mechanical agitation as seen in Table 3. The CSTR slurry reactor gave the best ethanol conversion among the suspended-beds, while the bubble fixed-bed gave the best conversion for the fixed-beds.

	A	B	C	D	E	F	G	H	I	J	K	L
Reaction 1	-1	-1	1	1								
Reaction 2		-1	-1	1	1							
Reaction 3												
Reaction 4												
Reaction 5												
Reaction 6												
Reaction 7												
Reaction 8												
Reaction 9												
Reaction 10												

For each reaction: use '-' for reactants and '+' for product components

DISPLAY EXIT

Fig.S4.S Reaction stoichiometry input screen

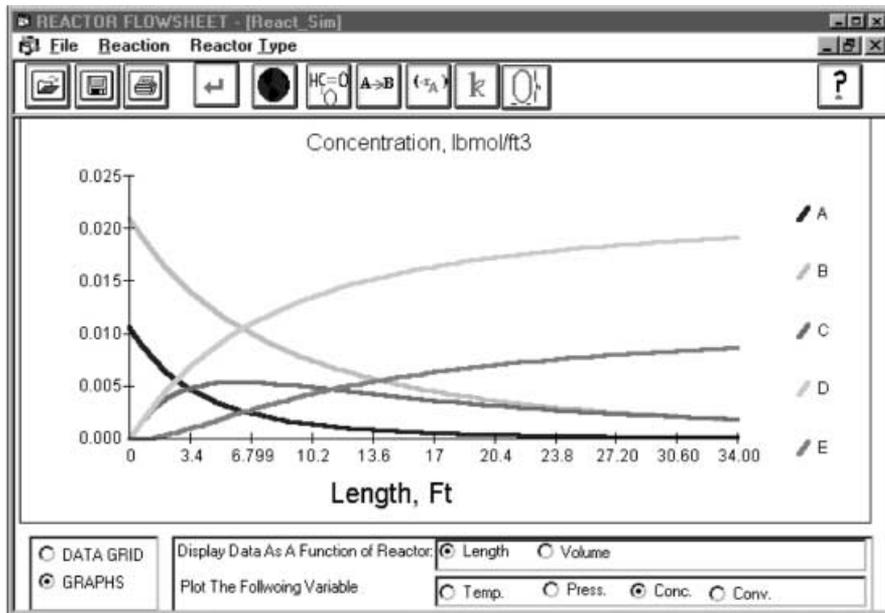


Fig.S5.S An illustration of the graphical output of ReaCat program

Table S1.2 Parameters and operating conditions for the oxidation of ethanol

Parameter or operating condition	
Catalyst particle diameter (cm)	Fixed-beds (trickle-bed and bub le fixed-bed) = 0.5 Suspended-beds (slurry and fluidized-beds) = 0.05
Catalyst load (g/cm ³)	Fixed-beds = 1.04 Suspended-beds = 0.1
Reactor diameter (cm)	20
Gas flow rate (cm ³ /s)	3140.0
Liquid flow rate (cm ³ /s)	62.8
Ethanol concentration in liquid phase at inlet (mol/cm ³)	4 × 10 ⁻⁴
Oxygen concentration at saturation (mol/cm ³)	4.2 × 10 ⁻⁶
Molecular diffusivity (cm ² /s)	4.7 × 10 ⁻⁵
Effective diffusivity (cm ² /s)	4.16 × 10 ⁻⁵
Catalyst density (g/cm ³)	1.2

Table S1.3 Mass transfer coefficients and catalytic effectiveness factor

Reactor	Catalytic effectiveness factor	G-L mass transfer coefficient (1/s)	Liquid phase dispersion coefficient (cm ² /s)	L-S mass transfer coefficient (1/s)
Trickle-bed	0.13	0.02	0.3266	0.0276
Bub le fixed-bed	0.13	0.144	0.9977	0.0408
CSTR slurry	0.799	1.05–1.45	–	1.14
Bub le slurry	0.799	0.02677	43.4	0.0952
Three-phase fluidized-bed	0.799	0.252	47.9	0.1

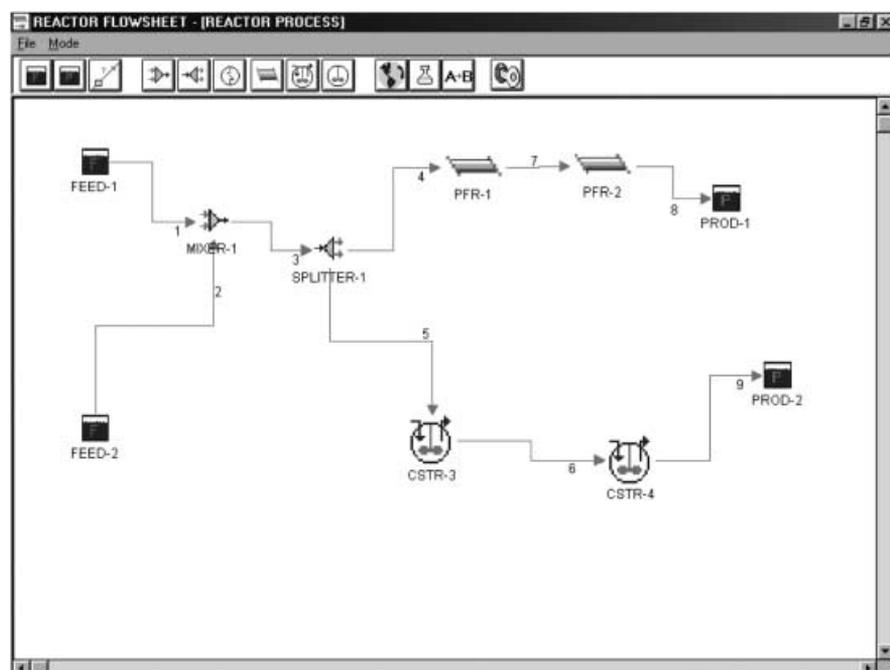


Fig. S6.5 Reactor flow-sheeting

This illustration of the use of the simulation package for these calculations demonstrates the significant capability to handle a very complex set of equations in a very effective and time-saving manner. Other examples where simulation results were compared against experimental data have also been illustrated (Salehi 1994).

Conclusion

A multi-phase catalytic reactor simulator has been developed. The simulation package has models to design the following reactor types: plug flow, CSTR, batch, catalytic

fixed-bed, catalytic fluidized-bed, gas-liquid stirred tank, trickle-bed, three-phase fixed bub le-bed, bub le slurry column, CSTR slurry, three-phase fluidized-bed. Power-law reaction rates for the Langmuir-Hinshelwood models are included. It is equipped with correlations to estimate the external mass transfer effects (gas-liquid and liquid-solid) and dispersion coefficients. Estimation of the catalytic effectiveness factor to account for the intra-particle resistance is also included. Isothermal and non-isothermal/nb-adiabatic conditions with multi-reaction systems with up to 30 reactions and 6 components are permitted.

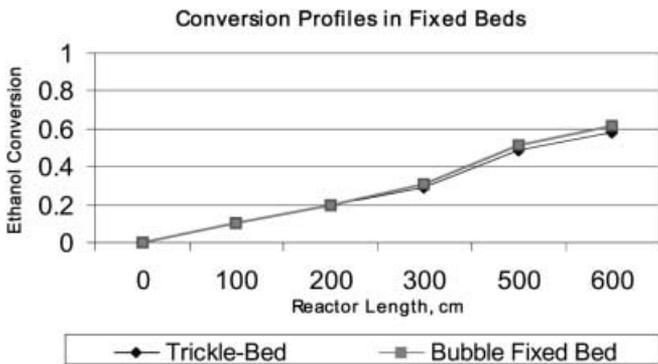


Fig. 7. Conversion of ethanol in three-phase fixed-beds

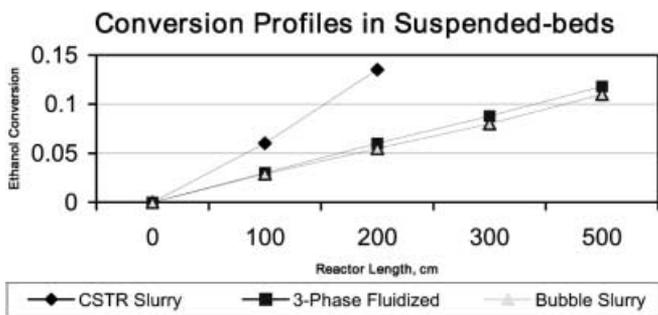


Fig. 8. Conversion of ethanol in three-phase suspended-beds

Reactor hydrodynamics such as pressure drop, power consumption, catalytic wetting factor, and flow regimes may also be predicted.

References

Achwal SK, Stepanek JB (1976) Holdup profiles in packed beds. *Chem Eng J* 2:69-75b

Akita SK, Yoshida S (1974) Bubble size, interfacial area, and liquid-phase mass transfer coefficient in bubble column. *Ind Eng Chem Process Des Dev* 13:84-91b

Baldi G, Gonti R, Salaria S (1974) Catalytic oxidation of formic acid in water: Interparticle diffusion in liquid-filled pores. *Chem Eng Sci* 33:21-25b

Berns L, Lidfelt J, Schoon NH (1976) Mass transfer and scale-up in batch hydrogenation. *J Appl Chem Soc* 463-466b

Broadhurst S, Becker H (1975) Onset of fluidization and slugging in beds of uniform particles. *Am Inst Chem Eng J* 21:238-247b

Calderbank PH (1958) Physical rate processes in industrial fermentation. Part I: Interfacial area in gas-liquid contacting with mechanical agitation. *Trans Inst Chem Eng* 36:443-446b

Charpentier JC (1981) Mass transfer rates in gas-liquid absorbers and reactors. *Adv Chem Eng* 1:12-133b

Chu JC, Kalil S, Sweteroth SW (1953) Mass transfer in fluidized bed. *Chem Eng Prog* 49:141-149b

Dakshinamurthy S, Subrahmanyam SCCV, Kameswarar R (1974) Studies of gas-liquid mass transfer in gas-liquid fluidized beds. In: Angelino H et al (eds) Fluidization and its applications. CEPADUES, Toulouse

Deckwer SWD, Burchhart R, Zool SG (1974) Mixing and mass transfer in tall bubble columns. *Chem Eng Soc* 29:2177-2188b

Dhanuka SVR, Stepanek JB (1980) Gas-liquid mass transfer in three-phase fluidized bed. In: Matson JR (ed) Fluidization. Plenum, New York

Dharwadkar SA, Sylvester SD (1977) Liquid-solid mass transfer in trickle-bed reactors. *Am Inst Chem Eng J* 23:940-944b

El-Temtamy SA, El-Sharnoubi SYO, El-Halwagi SM (1979) Liquid dispersion in gas-liquid fluidized beds. *Chem Eng J* 18:151-172b

Ellman SM, Midoux SG, Wild SA, Laurent SA, Charpentier JC (1988) A new, improved pressure drop correlation for trickle-bed reactors. *Chem Eng Sci* 43:2201-2206b

Ellman SM, Midoux SG, Wild SA, Laurent SA, Charpentier JC (1990) A new, improved liquid holdup correlation for trickle-bed reactors. *Chem Eng Sci* 45:1677-1683b

Fair JR (1967) Designing gas-sparged reactors. *Chem Eng* 74:67-72b

Froment SGF, Bischoff KB (1979) Chemical reactor analysis and design. Wiley, New York

Fukushima S, Kusaka S (1979) Gas-liquid mass transfer and hydrodynamic flow in packed column with cocurrent upward flow. *J Chem Eng Jpn* 2:706-713b

Goto S, Smith JM (1975) Trickle-bed reactor performance. Part I: Holdup and mass transfer effects. *Am Inst Chem Eng J* 21:706-720b

Govindarao SMH, Murthy SKY (1975) Liquid-phase hydrogenation of aniline in a trickle-bed reactor. *J Appl Chem Biotechnol* 25:169-181b

Harris JL, Norman JR (1972) *Ind Eng Chem Process Des Dev* 11:564b

Hedge SC (1999) Simulation for pollution prevention: gas-liquid reactors and sulfuric acid alkylation process. MSEE thesis, Lamar University

Hochman JM, Seffron S (1969) Two-phase concurrent downflow in packed beds. *Ind Eng Chem Fundam* 8:63b

Horio S, Nonaka A (1987) A generalized bubble diameter correlation for gas-solid fluidized beds. *Am Inst Chem Eng J* 33:1865-1871b

Kale S, S Chaudhari SRV, Ramachandran PA (1981) Butylenolysis: kinetic study. *Ind Eng Chem Prod Res Dev* 20:309-314b

Kim SD, Baker CG, Bergougnou M (1975) Phase holdup characteristics of three-phase fluidized beds. *Can J Chem Eng* 53:134-139b

Kobayashi S, Saito S (1965) Solid-liquid mass transfer in bubble columns. *Kagaku Koide* 2:10b

Kunii D, Levenspiel O (1969) Fluidization engineering. Wiley, New York

Larkins RP, White RR, Jeffery DW (1961) Two-phase concurrent flow in packed beds. *Am Inst Chem Eng J* 7:231-239b

Lee S, Sherrard SA, Buckley S (1974) Optimum particle size in three-phase fluidized-bed reactor. In: Angelino H et al (eds) Fluidization and its applications. CEPADUES, Toulouse

Luong SH, Volesky S (1979) Mechanical power requirements of gas-liquid agitated systems. *Am Inst Chem Eng J* 25:893-895b

Mangartz KH, Pilhofer S (1981) Interpretation of mass transfer measurements in bubble columns considering dispersion of both phases. *Chem Eng Sci* 36:1069-1077b

Maseller R (1970) Bubble columns. *Br Chem Eng* 15:1297-1366b

Michels J, Miller S (1962) Power requirements of gas-liquid agitated systems. *Am Inst Chem Eng J* 8:262-266b

Michell RW, Furzer S (1972) Mixing in trickle flow through packed beds. *Chem Eng J* 4:53-63b

Ostergaard S (1974) Gas-liquid-particle operation in chemical reaction engineering. *Adv Chem Eng* 7:1-137b

Pike RW, Hopper JR, Saleh J, Saws CL, Hertwig TA, Chen X, Selang K (1998) An advanced process analysis system for pollution prevention. In: Proceedings of Third International Conference on Foundations of Computer Aided Process Operations, Snowbird, Utah, 5-10 July. A.I. Chem Symposium Series, No 20, Vol 94, pp 421-427b

Ramachandran PA, Chaudhari SRV (1983) Three-phase catalytic reactors. Gordon and Breach, London

Reiss LP (1967) Cocurrent gas-liquid contacting in packed columns. *Ind Eng Chem Process Des Dev* 6:486-499

Saleh JM (1994) Computer simulation of three-phase catalytic gas-liquid reactions. Doctoral Dissertation, Lamar University, Beaumont, Texas

Sano S, Yamaguchi N, Adachi S (1974) Mass transfer coefficients for suspended particles in agitated vessels and bubble columns. *J Chem Eng Jpn* 7:255-261

Sato S, Hirose S, Takahashi S, Toda S (1973) Pressure loss and liquid holdup in packed-bed reactor with cocurrent gas-liquid downflow. *J Chem Eng Jpn* 6:147-152

Shah S (1979) Gas-liquid-solid reactor design. McGraw-Hill, New York

Specchia V, Baldi G (1979) Heat transfer in trickle-bed reactors. *Chem Eng Commun* 3:483-488

Specchia V, icardi S, Gianetto S (1978) Absorption in packed towers with cocurrent flow. *Am Inst Chem Eng J* 20:646-653b

- StiegelSGJ, ShahSYTS**(1977)Backmixingandliquidholdupin gas-liquidcocurrentupflowpackedcolumns.IndEngChemProcess DesDev16:37-43b
- TarhanSMO** (1979)Catalyticreactor design.McGraw-Hill, New Yorkb
- TelangSKS** (1996)Advancedprocessanalysis system.MSEBThesis, ChemicalEngineeringDepartment, LouisianaStateUniversityb
- TsutsumiSA, KimSYH, Togawa S, YoshidaSKS**(1987)Classificationof three-phase reactors.Sadhanal0:247-259b
- TurpinJL, HuntingtonRLS**(1967)Predictionof pressure dropfor two-phase, two-componentcocurrentflowinpacked beds.AmbInstb ChemEngj13:1196-1202b
- VanDierendonckSLS**(1970)Vergrottingsregelsvoor gasbelwassers. Ph.D.Thesis, TwenteUniversity, Netherlandsb
- VanKrevelenSDW, KrekelsJTC**(1948)Rateof dissolutionof solid substances.PartI.: physicaldissolution.Recl Trav Chim Pays-Bas 67:512b
- WaghchoureS** (1999)Simulationoftwo-phasecatalyticfluidized bed reactorsfor pollution prevention.MSEBThesis, LamarUniversity, Beaumont, Texasb
- YamashitaF, Aeon HS**(1975)Gas holdupin bubblecolumns. J Chem Eng Jpn18:334b
- YungSCN, WongSCW, ChangeSCL**(1979)Gas holdup and aerated power consumption in mechanically stirred tanks. Can J Chem Eng 57:672-677b